Statistics of dynamic polarization speckle generated from a moving rough-surfaced retardation plate

PROCEEDINGS OF SPIE

SPIEDigitalLibrary.org/conference-proceedings-of-spie

Statistics of dynamic polarization speckle generated from a moving rough-surfaced retardation plate

Ma, Ning, Hanson, Steen, Takeda, Mitsuo, Wang, Wei

Ning Ma, Steen G. Hanson, Mitsuo Takeda, Wei Wang, "Statistics of dynamic polarization speckle generated from a moving rough-surfaced retardation plate," Proc. SPIE 11369, Fourteenth International Conference on Correlation Optics, 1136902 (6 February 2020); doi: 10.1117/12.2540027

Event: Fourteenth International Conference on Correlation Optics, 2019, Chernivtsi, Ukraine

Statistics of dynamic polarization speckle generated from a moving rough-surfaced retardation plate

Ning Ma [a,b], Steen G. Hanson [c], Mitsuo Takeda [d] and Wei Wang [a*]
[a] Institute of Photonics and Quantum Sciences, School of Engineering and Physical Science, Heriot-Watt University, Edinburgh, EH14 4AS, United Kingdom
[b] Genius pros, 59 Shixiang West Rd. Building B, Floor13 Hangzhou, Zhejiang, 310030, China
[c] Department of Photonics Engineering, DTU Fotonik, P. O. Box 49, DK-4000 Roskilde, Denmark
[d] Center for Optical Research and Education (CORE), Utsunomiya University, 7-1-2 Yoto, Utsunomiya, Tochigi 321-8585, Japan

ABSTRACT

Laser speckle has received extensive studies in its basic properties and wide applications. In the majority of research on speckle phenomena, these random optical fields have been treated as scalar optical fields, and the main interest has been in the statistical properties together with applications of the intensity distribution of the speckle patterns. In recent years, increasing attention has been paid to the statistical properties of random electric vector fields referred to as polarization speckle with spatially varying polarization state. Statistical phenomena of random electric vector fields with their close relevance to the theories of speckles, polarization and coherence theory have come to attract emerging interest due to their importance in a variety of areas for practical applications such as biomedical optics, remote sensing, astronomical observation and optical metrology.

In this paper, we investigate the dynamic polarization speckle generated by a moving rough-surfaced retardation plate and present an exact analytical expression for the space-time lagged correlation for the stochastic fields within the framework of ABCD matrix theory (Canonical Transforms). General expressions are derived for the spot size, the mean polarization speckle size, the temporal coherence length, and the peak shift of the temporal correlation. Some interesting phenomena associated with dynamic polarization speckle have been predicted including polarization speckle boiling and polarization speckle translation. A general description of these phenomena has been given for arbitrary complex-valued ABCD optical systems.

Keywords: coherence, polarization, polarization speckle, statistical optics, ray matrices, canonical transforms.

1. INTRODUCTION

When a moving diffuse scattering object, for example a plate, is illuminated by a coherent laser source, the generated laser speckle usually appears as twinkling “particles” on the observation screen. The statistics of the dynamic speckle pattern mainly depends on the structural characteristics of the plate surface, the motion of the modulation plate, and the beam propagation system. Based on these relations, the speckle shape and dynamic features are adopted as a popular measurement method in non-destructive inspection for object motion, surface roughness, vibration, displacement, velocity, and rotation[1-6].Both theoretical and experimental analysis of the speckle with spatial variation of polarization states, usually named as polarization speckle[7], is carried out in recent years associated with propagation studies [8-17]. This is significantly different from the conventional scalar laser speckle research simply treating the field as a bundle of rays with uniform polarization. Here, the evolution of polarization during propagation will be included as well as the evolution of coherence. A rough-surfaced retardation plate was applied as a depolarizer in recent research of polarization speckle[18], and the statistical properties of the corresponding polarization speckle is presented.

In this paper, we will consider the moving motion of plate, and analyse the time-logged dynamic statistical properties of the generated speckle in the form of the 2×2 time-lagged beam coherence and polarization matrix as a continuation and extension of previous work. Its impact on the shape features of speckle, like the spot size, the mean polarization speckle

* w.wang@hw.ac.uk Tel: +44 (0) 131 451 3141; Fax: +44 (0) 131 451 3129

Fourteenth International Conference on Correlation Optics, edited by Oleg V. Angelsky, Proc. of SPIE Vol. 11369, 1136902 · © 2020 SPIE
CCC code: 0277-786X/20/$21 · doi: 10.1117/12.2540027

size, the temporal coherence length, and the peak shift of the temporal correlation will be illustrated as well. Some interesting phenomena like the polarization speckle boiling and polarization speckle translation will be discussed for arbitrary complex-valued ABCD optical systems. This research of polarization speckle is expected to facilitate potential metrological applications in medicine, biology or industry.

2. MODULATION BEHAVIOR OF MOVING ROUGH-SURFACED RETARDATION PLATE TO INCIDENT BEAM

The system used to examine the dynamic statistical properties of electric field modulated by a moving rough-surfaced retardation plate is shown in Fig. 1.

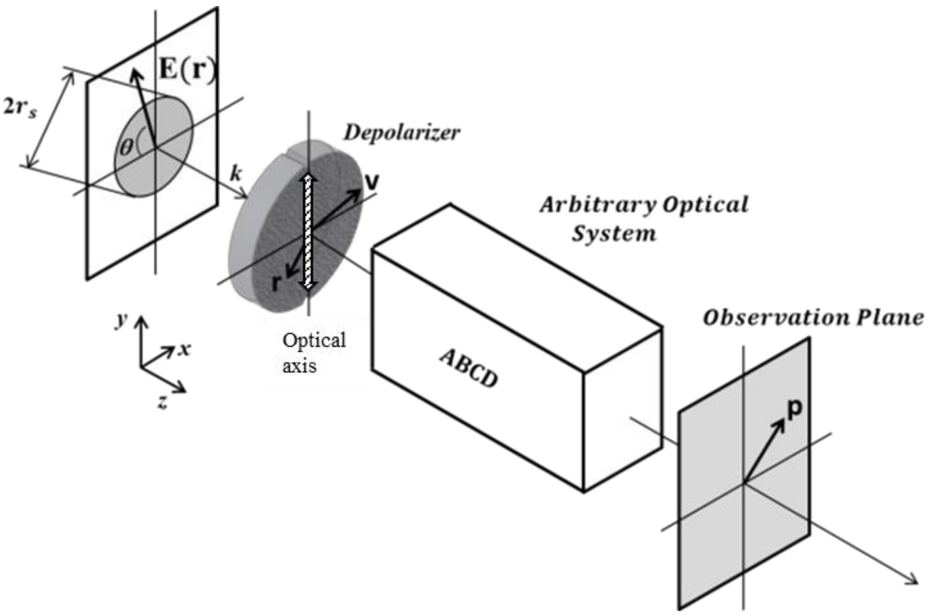

Figure 1. Schematic of the setup for obtaining the dynamic statistical properties of polarization speckle through an ABCD optical systems.

An incident beam composed of two complex components of the electric vector $\mathbf{E}^i(\mathbf{r},t)=\{\tilde{E}_x^i(\mathbf{r},t),\tilde{E}_y^i(\mathbf{r},t)\}$ of width r_s and wave vector $\vec{k}$ is incident on the rough-surfaced retardation plate at time t. The plate employed as a depolarizer is moving with a velocity vector $\mathbf{v}=\{v_x,v_y\}$ within the plane perpendicular to the *z*-axis, and its optical axis indicated by a line connecting the notches will be aligned along the $\hat{y}$ axis. Therefore, for the incident field $\mathbf{E}^i$ before, and the transmission field $\mathbf{E}^t$ after the depolarizer presented by the superscripts i or t, respectively, their relationship $\mathbf{E}^t=\mathbf{E}^i\mathbf{T}$ is governed by the transmission matrix $\mathbf{T}$[19]

$$\mathbf{T}(\mathbf{r})=\begin{pmatrix} e^{-j\varphi_x(\mathbf{r})} & 0 \\ 0 & e^{-j\varphi_y(\mathbf{r})} \end{pmatrix}=\begin{pmatrix} e^{-j\left[d(\mathbf{r})k(n_x-1)\right]} & 0 \\ 0 & e^{-j\left[d(\mathbf{r})k(n_y-1)\right]} \end{pmatrix}, \tag{1}$$

where $\varphi_m(\mathbf{r})=d(\mathbf{r})k(n_m-1)$, $(m=x,y)$ is the effective phase delay for the $\hat{x}$ or $\hat{y}$ components of the electric fields, k is the wavenumber of light in vacuum, n_m $(m=x,y)$ denotes the refractive indices of the birefringent material, j is the imaginary unit, and $d(\mathbf{r})$ is the local thickness. The relative phase shift between the two orthogonal components $\Delta=k(n_y-n_x)d(\mathbf{r})$ of the modulated field $\mathbf{E}^t(\mathbf{r})$ is proportional to the local thickness of the depolarizer, and will vary with the local shift. Thus, random polarization transformation is introduced successfully. For the sake of simplicity in the derivation, we will assume the statistics of the surface to be space and time independent, i.e., stationary and homogeneity in the micro-structure are invoked. The intensity transmission coefficient of the moving plate is assumed to be equal to unity.

For this moving depolarizer, the dynamic statistical properties of modulated fields $\mathbf{E}^t$ depending on the incident field and plate structure could conveniently be illustrated by a 2×2 time-lagged mutual coherence matrix[20,21] of field $\mathbf{E}^t$ at point $\mathbf{r}_1$ and point $\mathbf{r}_2$ with time-lag τ :

$$\begin{aligned}\mathbf{W}^t(\mathbf{r}_1,\mathbf{r}_2;\tau) &= \begin{pmatrix} \left\langle \tilde{E}_x^{t*}(\mathbf{r}_1,t)\tilde{E}_x^t(\mathbf{r}_2,t+\tau)\right\rangle & \left\langle \tilde{E}_x^{t*}(\mathbf{r}_1,t)\tilde{E}_y^t(\mathbf{r}_2,t+\tau)\right\rangle \\ \left\langle \tilde{E}_y^{t*}(\mathbf{r}_1,t)\tilde{E}_x^t(\mathbf{r}_2,t+\tau)\right\rangle & \left\langle \tilde{E}_y^{t*}(\mathbf{r}_1,t)\tilde{E}_y^t(\mathbf{r}_2,t+\tau)\right\rangle \end{pmatrix} \\ &= \begin{pmatrix} W_{xx}^i(\mathbf{r}_1,\mathbf{r}_2)\left\langle e^{j[\varphi_x(\mathbf{r}_1,t)-\varphi_x(\mathbf{r}_2-\tau\mathbf{v},t)]}\right\rangle & W_{xy}^i(\mathbf{r}_1,\mathbf{r}_2)\left\langle e^{j[\varphi_x(\mathbf{r}_1,t)-\varphi_y(\mathbf{r}_2-\tau\mathbf{v},t)]}\right\rangle \\ W_{yx}^i(\mathbf{r}_1,\mathbf{r}_2)\left\langle e^{j[\varphi_y(\mathbf{r}_1,t)-\varphi_x(\mathbf{r}_2-\tau\mathbf{v},t)]}\right\rangle & W_{yy}^i(\mathbf{r}_1,\mathbf{r}_2)\left\langle e^{j[\varphi_y(\mathbf{r}_1,t)-\varphi_y(\mathbf{r}_2-\tau\mathbf{v},t)]}\right\rangle \end{pmatrix}.\end{aligned} \tag{2}$$

where the asterisk * means complex conjugate, and angular brackets $\langle\cdots\rangle$ denote ensemble average.

In derivation of Eq. (2) we have made use of the statistical independence of the incident field's coherence property and the depolarizer's correlation property. For this plate moving with a constant velocity $\mathbf{v}$ normal to the direction of incidence of the illuminating beam, the time evolution of the local thickness is $d(\mathbf{r},t+\tau)=d(\mathbf{r}-\tau\mathbf{v},t)$. The elements of the coherence matrix in Eq. (2) is closely related to the characteristic function of the corresponding random variable $\Delta\varphi_{lm}(\mathbf{r}_1,\mathbf{r}_2;\tau)=\varphi_l(\mathbf{r}_1,t)-\varphi_m(\mathbf{r}_2-\tau\mathbf{v},t)$, $(l,m=x,y)$ which can be written as

$$\begin{aligned}&\left\langle \exp\left\{ j\Delta\varphi_{lm}(\mathbf{r}_1,\mathbf{r}_2;\tau)\right\}\right\rangle \\ &=\exp\left\{-\frac{k^2\left[(n_l-1)^2+(n_m-1)^2\right]\left\langle d^2(\mathbf{r})\right\rangle}{2}+\frac{k^2 2(n_l-1)(n_m-1)\left\langle d(\mathbf{r}_1)d(\mathbf{r}_2-\tau\mathbf{v})\right\rangle}{2}\right\}\end{aligned} \tag{3}$$

Here, a zero mean assumption of the thickness $\langle d(\mathbf{r})\rangle$ is introduced without loss of generality, since it has no effect on the polarization state scrambling of the incident beam. Furthermore, we take advantage of an isotropic Gaussian surface thickness correlation function and a Gaussian PDF for the statistics of the thickness for mathematical convenience, namely, let

$$\left\langle d(\mathbf{r}_1)d(\mathbf{r}_2)\right\rangle = {\sigma_d}^2\exp\left\{-\left|\Delta\mathbf{r}\right|^2/{r_d}^2\right\}, \tag{4}$$

where $\Delta\mathbf{r}=\mathbf{r}_1-\mathbf{r}_2$, and r_d is the lateral correlation length, and ${\sigma_d}^2$ is the local surface thickness variance. In the case of large surface roughness and small lateral correlation length to obtain a phase difference greater than 2π , i.e., $(\mathrm{n}_l-1)(n_m-1)k^2\sigma_d^2\gg(2\pi)^2$,($l,m=x,y$), Eq. (4) could be simplified:

$$\left\langle \exp\left\{ j\Delta\varphi_{lm,\tau}\right\}\right\rangle=\exp\left\{-\frac{k^2{\sigma_d}^2}{2}\left[\left(n_l-n_m\right)^2+2\left(n_l-1\right)\left(n_m-1\right)\frac{\left|\Delta\mathbf{r}+\tau\mathbf{v}\right|^2}{{r_d}^2}\right]\right.. \tag{5}$$

Thus the time-lagged mutual coherence matrix $\mathbf{W}^t$ could be derived by substituting Eq. (5) directly into Eq. (2), and the dynamic correlation properties of the polarization speckle determined by the plate surface features and motion state can be found. On the basis of this conclusion, further progress could be carried out to mathematically investigate the propagation of the dynamic polarization speckle through a complex ABCD system.

3. DYNAMIC POLARIZATION SPECKLE IN PROPAGATION

The prerequisite mathematical conclusions have been derived to analyse the propagation of the time-lagged mutual coherence matrix through an optical system. Under the paraxial approximation, the time-lagged mutual coherence matrix

$\mathbf{W}^o(\mathbf{p}_1,\mathbf{p}_2;\tau)$ for the field $\mathbf{E}^o$ arriving at the observation plane after passing through a complex ABCD optical system is connected to the time-lagged mutual coherence matrix of the modulated field $\mathbf{W}^t(\mathbf{r}_1,\mathbf{r}_2;\tau)$ by an integral formulation:

$$\mathbf{W}^o\left(\mathbf{p}_1,\mathbf{p}_2,\tau\right)=\iint_{\pm\infty}\mathbf{W}^t(\mathbf{r}_1,\mathbf{r}_2;\tau)G^*\left(\mathbf{p}_1,\mathbf{r}_1\right)G\left(\mathbf{p}_2,\mathbf{r}_2\right)d\mathbf{r}_1 d\mathbf{r}_2, \tag{6}$$

where the Green's function is given by

$$G(\mathbf{p},\mathbf{r})=-\frac{jk}{2\pi B}\exp\left\{-\frac{jk}{2B}\left(A|\mathbf{r}|^2-2\mathbf{r}\cdot\mathbf{p}+D|\mathbf{p}|^2\right)\right\}. \tag{7}$$

A, *B*, and *D* in Eq. (7) are the ABCD complex-valued matrix elements for the whole propagation system we discuss here. The resulting matrix is the multiplication of all the matrices for all the individual optical components included in this system, i.e., the lenses, free space propagations and aperture [22,23]. At the same time, identical refractive indices in the input and output plane are tacitly assumed for simplicity.

Without loss of generality, a spatially coherent Gaussian beam linearly polarized with an angle θ to the $\hat{x}$ axis will be applied as a typical example of an incident source for demonstration purpose in further discussion. Similar analysis procedure is applicable for the other kind of sources as well. Thus the coherence matrix for the linearly polarized Gaussian beam just in front of the depolarizer is given by

$$\mathbf{W}^i(\mathbf{r}_1,\mathbf{r}_2)=I_o\exp\left\{-\frac{|\mathbf{r}_1|^2+|\mathbf{r}_2|^2}{r_s^2}\right\}\begin{pmatrix}\cos^2\theta & \cos\theta\sin\theta\\ \cos\theta\sin\theta & \sin^2\theta\end{pmatrix}, \tag{8}$$

where I_o is the on-axis intensity of the incident field. The time-lagged mutual coherence matrix $\mathbf{W}^t(\mathbf{r}_1,\mathbf{r}_2;\tau)$ of the modulated field after the depolarizer is derived by substituting Eq. (5) and Eq.(8) into Eq. (2):

$$\mathbf{W}_{xx}^t=I_o\exp\left\{-(|\mathbf{r}_1|^2+|\mathbf{r}_2|^2)/r_s^2\right\}\cos^2\theta\exp\left\{-k^2\sigma_d^2(n_x-1)^2|\Delta\mathbf{r}+\tau\mathbf{v}|^2/r_d^2\right\}; \tag{9}$$

$$\mathbf{W}_{yy}^t=I_o\exp\left\{-(|\mathbf{r}_1|^2+|\mathbf{r}_2|^2)/r_s^2\right\}\sin^2\theta\exp\left\{-k^2\sigma_d^2(n_x-1)^2|\Delta\mathbf{r}+\tau\mathbf{v}|^2/r_d^2\right\}; \tag{10}$$

$$\mathbf{W}_{xy}^t=\mathbf{W}_{yx}^t=I_o\exp\left\{-(|\mathbf{r}_1|^2+|\mathbf{r}_2|^2)/r_s^2\right\}\sin\theta\cos\theta\exp\left\{-\tfrac{1}{2}k^2\sigma_d^2\left[(n_y-n_x)^2+2\left(n_x-1\right)\left(n_y-1\right)|\Delta\mathbf{r}+\tau\mathbf{v}|^2/r_d^2\right]\right\}. \tag{11}$$

We next consider the evolution of the statistical properties of the dynamic polarization speckle generated by the rough-surfaced retardation plate illuminated by the linearly polarized Gaussian beam during propagation. Usually, it is the amplitude of the coherence matrix elements that is of most interest in practical applications, because the intensity distribution in the observation plane can be observed easily in most cases. Hence, we derive the amplitude of the time-lagged coherence matrix after travelling through the ABCD system by substitution of Eqs.(9)-(11), into Eq. (6):

$$\left|\mathbf{W}^o\left(\mathbf{p}_1,\mathbf{p}_2,\tau\right)\right|=I_o\cos\theta\sin\theta$$
$$\begin{pmatrix}\cot\theta\left|W(\mathbf{p}_1,\mathbf{p}_2;\tau,\dfrac{r_d^2}{k^2\sigma_d^2\left(n_x-1\right)^2})\right| & \exp\left\{-\dfrac{k^2\sigma_d^2(n_x-n_y)^2}{2}\right\}\left|W\left(\mathbf{p}_1,\mathbf{p}_2;\tau,\dfrac{r_d^2}{k^2\sigma_d^2\left(n_x-1\right)\left(n_y-1\right)}\right)\right|\\ \exp\left\{-\dfrac{k^2\sigma_d^2(n_x-n_y)^2}{2}\right\}\left|W\left(\mathbf{p}_1,\mathbf{p}_2;\tau,\dfrac{r_d^2}{k^2\sigma_d^2\left(n_x-1\right)\left(n_y-1\right)}\right)\right| & \tan\theta\left|W\left(\mathbf{p}_1,\mathbf{p}_2;\tau,\dfrac{r_d^2}{k^2\sigma_d^2\left(n_y-1\right)^2}\right)\right|\end{pmatrix}, \tag{12}$$

where $W(\mathbf{p}_1,\mathbf{p}_2;\tau,\beta_{lm})$, $(l,m=x,y)$ for each matrix element is the result of the integral function with parameter r_{lm}^{η} and r_{lm}^{w} :

$$
\begin{aligned}
W_{lm}(\mathbf{p_1},\mathbf{p_2};\tau,\beta_{lm}) &= \frac{\beta_{lm}}{\left(r_{lm}^{\eta}\right)^2}\exp\left\{\frac{-\left|\Delta\mathbf{p}+A\mathbf{v}\tau\right|^2}{\left(r_{lm}^{c}\right)^2}\right\}\exp\left\{\frac{-\left(\left|\mathbf{p}_1\right|^2+\left|\mathbf{p}_2\right|^2\right)}{\left(r_{lm}^{w}\right)^2}\right\}\\
r_{lm}^{c} &= \left(4\,\mathrm{Im}\left[A^*B\right]\big/k+\beta_{lm}\,|A|^2\right)^{1/2}\\
r_{lm}^{w} &= \frac{|B|\,r_{lm}^{\eta}}{\left(-2\,\mathrm{Im}\left[B\right]^2+2\,\mathrm{Im}\left[A^*B\right]\mathrm{Im}\left[D^*B\right]+\frac{k\beta_{lm}}{2}\left(|A|^2\,\mathrm{Im}\left[B^*D\right]-\mathrm{Im}\left[AB\right]\right)\right)^{1/2}}\\
\beta_{lm} &= \frac{r_d^{\;2}}{k^2\sigma_d^2\left(n_l-1\right)\left(n_m-1\right)}.
\end{aligned}
\tag{13}
$$

In the derivation of Eq. (13), the given intensity radius and radius of curvature of the incident beam are omitted on purpose, and can be compensated by including a limiting aperture and a lens as the first element(s) of the propagation system, while calculating the total ABCD matrix.

Equations (12) and (13) providing the analytic results for the propagation of the time-lagged mutual coherence matrix through a complex ABCD optical system is the main conclusions of this section. By utilizing these analytical results for propagation through arbitrary optical system, the evolution of the corresponding dynamic statistical properties and shape features of the dynamic polarization speckle in any observation plane could be analysed for a moving depolarizer illuminated by a linearly polarized Gaussian electromagnetic beam. Some interesting dynamic polarization speckle phenomena will be revealed in the following discussion.

Consider the *x*-wave component of the propagated field and the corresponding dynamic speckle generated: If the $\Delta\mathbf{p}=\mathbf{p_1}-\mathbf{p_2}$ and τ are set to zero, matrix element $W^{o}{}_{xx}(\mathbf{p},\mathbf{p};0)$ of Eq. (12) in Gaussian form will illustrate the beam intensity distribution of the *x*-wave element. The $1/e^2$ radius r_{xx}^{w} demonstrates the illuminated spot region of the *x*-wave element on the observation screen. Likewise, the illuminated spot region size of the *y*-wave element, which is distinct from the one in the *x*-direction, is correspondingly indicated by the $1/e^2$ radius r_{yy}^{w} of matrix element $W_{yy}^{o}(\mathbf{p},\mathbf{p};0)$. The difference between these two wave elements' beam shapes is directly caused by the differences of β_{lm} ($l,m=x,y$) in $W^{o}{}_{xx}(\mathbf{p},\mathbf{p};0)$ and $W_{yy}^{o}(\mathbf{pp};0)$. As one of the significantly important conclusions of this paper, this illustrates the effect of the depolarizer's birefringence on field modulation behaviour causing orientation dependence. Consequently, this indicates the necessity of the tensor field expression in this research instead of the conventional scalar field expression. Moreover, in the absence of time lag $\tau=0$, the r_{xx}^{η} and r_{yy}^{η} in $W_{mm}^{o}(\Delta\mathbf{p},0)$ ($m=x$ or y) as denominator of $\Delta\mathbf{p}$'s Gaussian functions measures the lateral correlation length of for the *x*- and *y*-wave elements respectively, and specifies the difference between their speckle sizes. Therefore, the disparities of speckle shape features between the *x*- and *y*-wave elements are revealed.

If non-zero time lag τ is introduced, the differences in dynamic features of polarization speckle embodied in the mathematical expression of matrix elements in Eq. (12) and (13) will be investigated as well. When points distance $\Delta\mathbf{p}$ is zero, the denominators $r_{lm}^{\eta}/(A\mathbf{v})$, ($l,m=x,y$) of Gaussian functions of τ in the corresponding $W_{lm}^{o}(\Delta\mathbf{p},0)$ point out the temporal correlation length τ_{lm}^{c} between the propagated field's l and m wave elements:

$$
\tau_{xx}^{c}=\frac{\left(4k\,\mathrm{Im}\left[\frac{B}{A}\right]+\frac{r_d^2}{\sigma_d^{\;2}\left(n_x-1\right)^2}\right)^{1/2}}{k|\mathbf{v}|};
\tag{14}
$$

$$\tau_{yy}^{c}=\frac{\left(4k\,\mathrm{Im}\left[\frac{B}{A}\right]+\frac{r_d^2}{\sigma_d{}^2\left(n_y-1\right)^2}\right)^{1/2}}{k\left|\mathbf{v}\right|};\tag{15}$$

$$\tau_{xy}^{c}=\tau_{yx}^{c}=\frac{\left(4k\,\mathrm{Im}\left[\frac{B}{A}\right]+\frac{r_d^2}{\sigma_d{}^2\left(n_x-1\right)\left(n_y-1\right)}\right)^{1/2}}{k\left|\mathbf{v}\right|}.\tag{16}$$

Eq. (14)-(16) present the generalization of the transition times for speckle engendered by the *x-x*, *y-y*, and *x-y* wave components, respectively.

This being different from the polarized case shows the importance of the derived results.

If we normalize the matrix element, $W_{lm}^{o}(\mathbf{p_1},\mathbf{p_2},\tau)\ \ (l,m=x,y)$ in Eq. (12) to its corresponding square root at points $\mathbf{p_1}$ and $\mathbf{p_2}$ i.e., $W_{lm}^{o}(\mathbf{p_1},\mathbf{p}_1,0)$ and $W_{lm}^{o}(\mathbf{p_2},\mathbf{p}_2,0)$, then we get the normalized coherence expression

$$\gamma_{lm}\left(\mathbf{p_1},\mathbf{p_2},\tau\right)=\exp\left\{\frac{-\left|\Delta\mathbf{p}+\mathrm{Re}\left[A\right]\mathbf{v}\tau\right|^2}{\left(r_{lm}^{\eta}\right)^2}\right\}\exp\left\{\frac{-\left|\mathrm{Im}\left[A\right]\mathbf{v}\tau\right|^2}{\left(r_{lm}^{\eta}\right)^2}\right\},\tag{17}$$

by which, more dynamic properties of polarization speckle can be extracted.

For far field propagation distance or in the Fourier plane of a Fourier transforming system ($\mathrm{Re[A]}\to 0$), Eq. (17) consist of Gaussian function of $\Delta\mathbf{p}$ and a Gaussian function of τ , being independent, thus indicating speckle decorrelation only without speckle displacement:

$$\gamma_{lm}\left(\mathbf{p_1},\mathbf{p_2},\tau\right)=\exp\left\{\frac{-\left|\Delta\mathbf{p}\right|^2}{\left(r_{lm}^{\eta}\right)^2}\right\}\exp\left\{\frac{-\left|\mathrm{Im}\left[A\right]\mathbf{v}\tau\right|^2}{\left(r_{lm}^{\eta}\right)^2}\right\}.\tag{18}$$

This is called speckle boiling [24], where speckle boiling of the x and y element could be observed in identical system structure. However, Eq. (18) also demonstrates different temporal correlation lengths depending on the polarization component.

On the other hand, when $\mathrm{Im[A]}\to 0$, (i.e. in the near field or in the image plane), Eq. (17) becomes

$$\gamma_{lm}\left(\mathbf{p_1},\mathbf{p_2},\tau\right)=\exp\left\{\frac{-\left|\Delta\mathbf{p}+\mathrm{Re}\left[A\right]\mathbf{v}\tau\right|^2}{\left(r_{lm}^{\eta}\right)^2}\right\}.\tag{19}$$

The closely related $\Delta\mathbf{p}$ and τ in the numerator of the Gaussian function illustrates the speckles moving as a whole. This characteristic speckle pattern is usually called speckle translation [24]. As shown in Eq.(19), the time required for any $W_{lm}^{o}(\mathbf{p_1},\mathbf{p_2},\tau)\ \ (l,m=x,y)$ to translate a fixed distance $\Delta\mathbf{p}$ equals $|\,\Delta\mathbf{p}\,/\,A\mathbf{v}\,|$, and hence the speed $\mathbf{v_s}$ of the speckles, is identical and is given by

$$\mathbf{v}_s=\mathrm{Re}[A]\mathbf{v}.\tag{20}$$

This means, although beam size and mean speckle size are different for $W_{lm}^{o}(\mathbf{p_1},\mathbf{p_2},\tau)$ generated by different wave components, that the translation of these speckles move with the same velocity. When we observe the entire field, any speckle separation due to polarization will not be observed.

4. CONCLUSIONS

In summary, we have examined the dynamic features of polarization speckle generated by a rough-surfaced depolarizer. Under the Gaussian assumption, we have presented a model for a moving rough-surfaced retardation plate acting as a depolarizer and have established a close relationship between the scattered electric fields' time-lagged mutual coherence matrix and the surface thickness fluctuations and motion of this birefringent depolarizer. By combining the time-lagged coherence matrix for polarization speckle together with the complex ABCD theory of wave propagation, we derived a general expression for the propagated time-lagged coherence matrix characterizing the dynamics and statistics of a propagating speckle field. Thus, the dynamic variation of the features of the propagated polarization speckle in the observation plane is revealed. In particular, we have shown the differences in the polarized speckle features, such as the mean spot size, the mean speckle size and the temporal coherence length for speckle elements $W_{lm}^{o}(\mathbf{p}_1, \mathbf{p}_2, \tau)$ $(l, m = x, y)$. In addition, the feasibility of generating both pure boiling and pure translation polarization speckle in an arbitrary observation plane has been demonstrated with a general description of the system prerequisite.

This analysis is expected to be helpful in the understanding of evolution of polarization speckle shape and motion features, and thus facilitate relevant theoretical and industrial applications.

5. REFERENCE

[1] Asakura, T., Takai, N., 'Dynamic laser speckles and their application to velocity measurements of the diffuse object', Appl. Phys. **25**(3), 179–194 (1981).

[2] Ruffing, B., 'Application of speckle-correlation methods to surface-roughness measurement: a theoretical study', J. Opt. Soc. Am. A **3**(8) (1986).

[3] Sirohi, R. S., Speckle Metrology Optical Engineering, JOUR, CRC Press, R. Sirohi, Ed., Marcel Dekker, Inc (1993).

[4] Dewhurst, R. J., Shan, Q., 'Optical remote measurement of ultrasound', Meas. Sci. Technol. **10**(11), R139–R168 (1999).

[5] Drain, L. E., 'The laser Doppler techniques', Chichester, Sussex, Engl. New York, Wiley-Interscience, 1980. 250 p. **1** (1980).

[6] Rose, B., Imam, H., Hanson, S. G., Yura, H. T.., Hansen, R. S., 'Laser-speckle angular-displacement sensor: theoretical and experimental study', Appl. Opt. **37**(11), 2119–2129 (1998).

[7] Wang, W., Hanson, S. G., Takeda, M., 'Statistics of polarization speckle: theory versus experiment', Ninth Int. Conf. Correl. Opt. Proc. SPIE **7388**(0), O. V. Angelsky, Ed., 738803-738803–738809 (2009).

[8] Wolf, E., 'Unified theory of coherence and polarization of random electromagnetic beams', Phys. Lett. A **312**, 263–267 (2003).

[9] Gori, F., Santarsiero, M., Vicalvi, S., Borghi, R., Guattari, G., Guattari, F. G. and M. S. and S. V. and R. B. and G., 'Beam coherence-polarization matrix', Pure Appl. Opt. J. Eur. Opt. Soc. Part A **7**, 941 (1998).

[10] James, D. F. V., 'Change of polarization of light beams on propagation in free space', J. Opt. Soc. Am. A **11**(5), 1641–1643, Optical Society of America (1994).

[11] Shirai, T., Wolf, E., 'Coherence and polarization of electromagnetic beams modulated by random phase screens and their changes on propagation in free space', J. Opt. Soc. Am. A **21**(10), 1907–1916 (2004).

[12] Hanson, S. G., Wang, W., Jakobsen, M. L., Takeda, M., 'Coherence and polarization of electromagnetic beams modulated by random phase screens and their changes through complex ABCD optical systems', J. Opt. Soc. Am. A **25**(9), 2338–2346 (2008).

[13] Angelsky, O. V., Polyanskii, P. V., Mokhun, I. I., 'Optical Measurements : Polarization and Coherence of Light Fields', [Modern Metrology Concerns], 263–317 (2012).

[14] Singh, R. K., Naik, D. N., Itou, H., Miyamoto, Y., Takeda, M., 'Characterization of spatial polarization fluctuations in scattered field', J. Opt. **16**(10), 105010, IOP Publishing (2014).

[15] Takeda, M., Wang, W., Hanson, S. G., 'Polarization speckles and generalized Stokes vector wave: a review', Proc. SPIE **7387**, A. Albertazzi Goncalves, Jr. and G. H. Kaufmann, Eds., 73870V–1–73870V–7 (2010).

[16] Scudieri, F., Bertolotti, M., Bartolino, R., 'Light scattered by a liquid crystal: a new quasi-thermal source', Appl. Opt. **13**, 181–185 (1974).

[17] Fercher, A. F., Steeger, P. F., 'First-order Statistics of Stokes Parameters in Speckle Fields', Opt. Acta Int. J. Opt. **28**(4), 443–448, Taylor & Francis Group (1981).
[18] Ma, N., Hanson, S. G., Takeda, M., Wang, W., 'Coherence and polarization of polarization speckle generated by a rough-surfaced retardation plate depolarizer', JOUR, J. Opt. Soc. Am. A **32**(12), 2346–2352, Optical Society of America (2015).
[19] Jones, R. C., 'A New Calculus for the Treatment of Optical Systems. I. description and discussion of the calculus', JOUR, J. Opt. Soc. Am. **31**(7), 488–93, OSA (1941).
[20] Mandel, L., Wolf, E., Optical Coherence and Quantum Optics, CAMBRIDGE Univ. (1995).
[21] Wolf, E., Introduction to the Theory of Coherence and Polarization of Light, book, CAMBRIDGE Univ., CAMBRIDGE UNIVERSITY (2007).
[22] Siegman, A. E., Lasers, misc, Mill Val., University Science Books (1986).
[23] Yura, H. T., Hanson, S. G., 'Optical beam wave propagation through complex optical systems', J. Opt. Soc. Am. A **4**(10), 1931–1948 (1987).
[24] Yura, H. T., Rose, B., Hanson, S. G., 'Dynamic laser speckle in complex ABCD optical systems', J. Opt. Soc. Am. A **15**(5), 1160–1165 (1998).